J Appl Electrochem (2010) 40:215–223
DOI 10.1007/s10800-009-0008-y

ORIGINAL PAPER

Protection of mild steel corrosion with new thia-derivative Salens in 0.5 M H_2SO_4 solution

M. G. Hosseini · H. Khalilpur · S. Ershad · L. Saghatforoush

Received: 25 May 2008 / Accepted: 11 February 2009 / Published online: 18 September 2009

Abstract The corrosion inhibition of mild steel in 0.5 M sulfuric acid by two newly synthesized Schiff bases namely, 4-X-2-{[2-(2-pyridin-2-yl-ethylsulfanyl) ethylimino] methyl}-phenol [X = $-NO_2$ (S_1) and –OMe (S_2)] has been investigated in the temperature range 298–318 K using Tafel polarization and electrochemical impedance spectroscopy (EIS) methods. The inhibition efficiency of both S_1 and S_2 increases with increase in inhibitor concentration. The variation in inhibition efficiency depends on the type of functional group substituted in the benzene ring. It was found that the presence of the methoxy group in the Schiff base (S_2) better facilitates the adsorption of molecules on the surface than is the case with S_1. Tafel polarization showed that both Schiff bases are mixed corrosion inhibitors. The Temkin isotherm was found to provide an accurate description of the adsorption behavior of the Schiff bases. Calculation of thermodynamic parameters such as ΔG^0_{ads}, ΔH^0_{ads} and ΔS^0_{ads} shows that the inhibitive action of the inhibitors is in the following order $S_1 < S_2$.

Keywords Schiff bases · Thia-derivative salens · Mild steel · Temkin adsorption · Electrochemical impedance spectroscopy

M. G. Hosseini (✉) · H. Khalilpur
Electrochemistry Research Laboratory, Department of Physical Chemistry, Chemistry Faculty, University of Tabriz, Tabriz, Iran
e-mail: mg-hosseini@tabrizu.ac.ir

S. Ershad
Department of Chemistry, Peyam-Nour University (PNU), Marand, Iran

L. Saghatforoush
Department of Chemistry, Peyam-Nour University (PNU), Khoy, Iran

1 Introduction

Acidic solutions are widely used for removal of undesirable scale and rust in many industrial processes. Inhibitors are generally used in these processes to control metal dissolution as well as the consumption of acid [1–3]. Nowadays, organic inhibitors perform this role well and a new series of them is being developed to replace inorganic compounds. Schiff bases—the condensation product of an amine and a ketone or aldehyde, and with $R_2C{=}NR–$ as general formula—are known examples of this category, and have been investigated for the inhibition of acid corrosion of mild steel [2, 3], copper [4], and aluminum [5].

Our previous studies have shown that aromatic Schiff bases are effective corrosion inhibitors in different corrosive media [2, 6–8]. As they have some atoms such as O and N with unpaired electrons and also the benzene ring in their structure, they have more than one center of chemical adsorption action and can form a stable chelate with metals. The greatest advantage of many Schiff base compounds is that they can be conveniently and easily synthesized from relatively inexpensive materials. The inhibition efficiency of Schiff bases is much greater than that of corresponding amines and aldehydes; this fact is attributable to the presence of a –C=N– group in the molecules [9]. The polar unit is regarded as the reaction center for the adsorption process. Thus, polar organic compounds are adsorbed on the metal surface, forming a charge transfer complex bond between their polar atoms and the metal. The size, orientation, shape, and electric charge on the molecule determine the degree of adsorption and hence the effectiveness of the inhibitor [10–16]. The previous considerations led us to synthesize the Schiff base molecules with structures depicted in Fig. 1, namely, (S_1) and (S_2), [17]. The introduction of a sulfur atom in

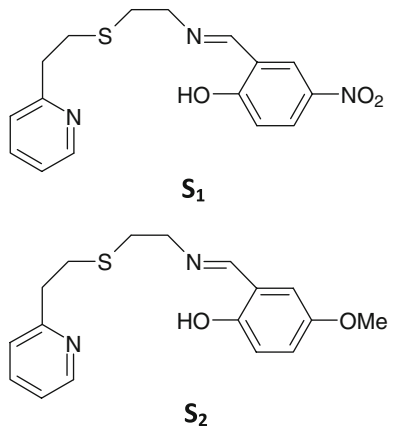

Fig. 1 Chemical structure of the Schiff bases S_1 and S_2

heterocyclic compounds containing nitrogen has been proved very good for inhibition of metal corrosion in acidic solutions [2, 4, 18–21].

The aim of this study is to investigate the corrosion inhibition effect of some newly synthesized thia-derivative Salens in 0.5 M H_2SO_4 solution in the temperature range 298–318 K using polarization and impedance techniques. The adsorption mechanisms of the new Schiff bases are investigated. Several isotherms are tested for their relevance in describing the adsorption behavior and differences in behavior are explained based on structural properties.

2 Experimental

2.1 Electrodes

Working electrodes were prepared using a mild steel plate with composition (in wt%) C 0.01, Si 0.35, P 0.018, Cr 0.04, Mo 0.03, Ni 0.017, Cu 0.02, Al 0.06, and Fe (balance). The samples were polished to mirror finish, using emery paper followed by aqueous alumina suspensions with particle sizes decreasing down to 0.05 μm. Platinum gauze and a saturated calomel electrode (SCE) were used as the counter and reference electrode, respectively. A Luggin capillary was employed for preventing potential deviation of the reference electrode. To obtain the stabilized open circuit potential (OCP), the samples were immersed for 30 min in the solution before EIS and Tafel polarization measurements. To be confident of the reproducibility, each measurement was performed three times in the same conditions and the mean results were chosen.

2.2 Inhibitors

All chemicals were of analytical reagent grade (Merck) and were used without further purification. Schiff bases with structures shown in Fig. 1 were synthesized according to the literature [17]. Briefly, a solution of 1 mmol of 2-pyridin-2-yl-ethylsulfanyl in 5 mL absolute ethanol was added to a solution of 1 mmol of salicylaldehyde in 5 mL absolute ethanol to give clear yellow or orange solutions, which were gently refluxed for about 60 min. Evaporation of the solution in vacuum, gave viscous ligands, S_1 and S_2 as microcrystals. The micro-crystals were filtered off, washed with 5 mL of cooled absolute ethanol and then re-crystalized from ethanol–chloroform solution (2:1, v/v). Inhibitor solutions were prepared in 0.5 mol dm^{-3} sulfuric acid with double distillated water, to which 5 vol.% methanol was added for solubility reasons.

2.3 Electrochemical impedance spectroscopy

An EG&G Princeton Applied Research Model 2245 potentiostat was used for electrochemical measurements. In the conventional three-electrode assembly, a Pt foil auxiliary electrode and a saturated calomel reference electrode (SCE) were used. After immersion of the specimen, prior to the impedance measurement, a stabilization period of 30 min was observed, which proved sufficient for the open circuit potential (Eoc) to attain a stable value. The alternating current frequency range extended from 10^5 to 10^{-2} Hz, with a 10 mV peak-to-peak sine wave as the excitation signal. Each impedance spectrum was simulated with the software "ZViewII" and the best fitting was achieved by applying a Randle's cell in which a capacitor (C_{dl}) is in parallel with a resistor (R_{ct}) and both are in series with the solution resistance (R_s).

2.4 Tafel polarization

The same equipment was used as for the impedance measurements, leaving the frequency response analyzer out of consideration for Tafel Polarization. Tafel polarization was performed within the potential range ±200 mV at a scan rate of 1 mV s^{-1}. All potentials are reported versus SCE.

3 Results and discussion

3.1 Electrochemical impedance spectroscopy

Figures 2 and 3 show a set of Nyquist plots of mild steel in 0.5 M H_2SO_4 in the absence and presence of various concentrations of the Schiff base S_1 at 313 K and S_2 at 298 K, respectively. The EIS results show that increasing the concentration of the inhibitor caused the values of charge transfer resistance to be shifted to higher values and this trend applies for both Schiff bases. Figure 4a shows a

typical fitting of simulated with experimental data (filled circles: experimented data, lines: simulated data); Fig. 4b is the equivalent circuit used for modelling of the

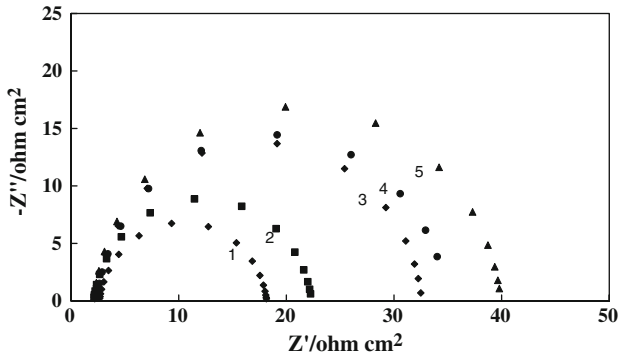

Fig. 2 Nyquist plots of mild steel in 0.5 M H_2SO_4 at 308 K in the presence of different concentrations (ppm) of S_1: (1) Bare, (2) 100, (3) 200, (4) 300 and (5) 400 ppm

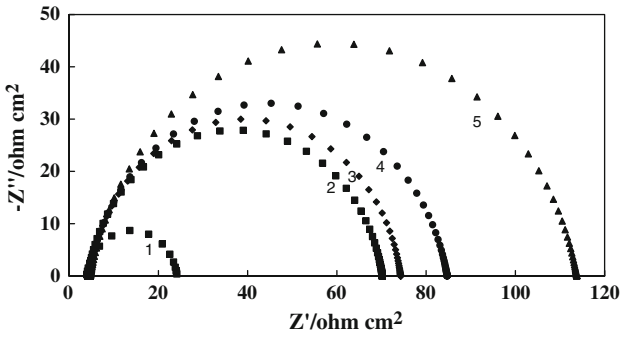

Fig. 3 Nyquist plots of mild steel in 0.5 M H_2SO_4 at 298 K, in the presence of different concentrations (ppm) of S_2: (1) Bare, (2) 100, (3) 200, (4) 300 and (5) 400 ppm

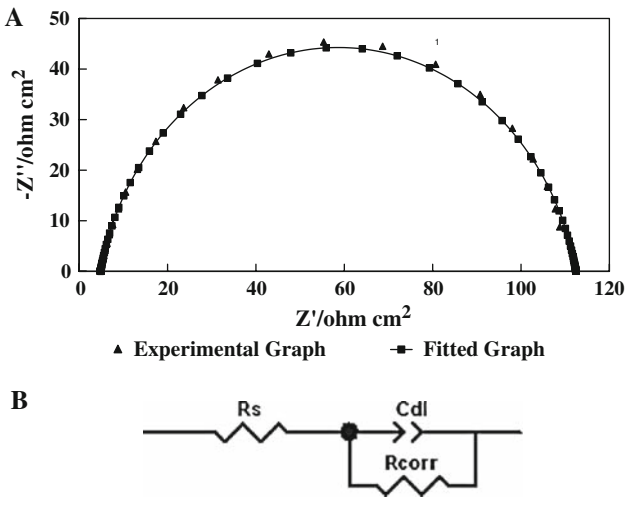

Fig. 4 **a** Nyquist plots of mild steel in 0.5 M H_2SO_4 at 308 K and the concentrations of S_2 is 300(ppm); *Filled triangles* experimented data, *Squares* fitted data; **b** The equivalent circuit used for modelling of the impedance spectra for both Schiff Bases S_1 and S_2

impedance spectra for both Schiff Bases S_1 and S_2. The impedance and admittance of a CPE are defined as follows [6]:

$$Z_{\text{cpe}} = \frac{1}{Y_0(j\omega)^n} \tag{1}$$

where Y_0 and n are frequency-independent parameters and $-1 \leq n \leq 1$. It is easily verified that this CPE shows purely resistive, capacitive, or inductive behavior when $n = 0$, 1 or -1, respectively. A constant phase element (CPE) was substituted for C_{dl}. This substitution was based on the depressed appearance of the recorded complex plane plots. Although a function of the above form allows very precise simulations of the measured impedance behavior, the parameters Y_0 and n cannot immediately be interpreted as familiar electrical parameter values.

Tables 1 and 2 show the impedance parameters of the Nyquist plots of the Schiff bases in different concentrations in the temperature range 298–318 K. Inhibition efficiencies $\eta_{\%Z}$ were calculated through the following equation:

$$\eta_{\%Z} = \frac{R_{\text{ct0}}^{-1} - R_{\text{ct}}^{-1}}{R_{\text{ct0}}^{-1}} \times 100 \tag{2}$$

where R_{ct0} and R_{ct} are values of the charge transfer resistance (Ω cm^2) observed in the absence and presence of inhibitor, respectively. With increasing inhibitor concentration, the inhibition efficiency ($\eta_{\%Z}$) is increased. Comparison of the data in Table 1 shows that with increasing temperature the inhibition efficiency decreases. As the inhibitor concentration increases, the R_{corr} values increase, but the C_{dl} values tend to decrease. The decrease in C_{dl} is due to adsorption of inhibitor on the metal surface. This phenomenon is commonly found in cases where adsorption at the metal/electrolyte interface occurs, as solvent molecules (in this case water, with high dielectric constant) are replaced with molecules with far less pronounced dielectric properties. If molecular adsorption at the metal/solution interface is essentially the mechanism through which the corrosion inhibition occurs, several adsorption isotherms can be tested for their relevance in describing the interaction between inhibitor and the metal surface, at least on a phenomenological level (see Sect. 3.4).

3.2 Tafel polarization

Figures 5 and 6 show Tafel polarization measurements for mild steel in 0.5 M H_2SO_4 in the absence and presence of the Schiff base S_1 and S_2, respectively. Tables 3 and 4 show the polarization parameters for corrosion of mild steel in the presence of different concentrations of the Schiff bases. The corrosion inhibition efficiency ($\eta_{\%P}$) is defined as:

Table 1 Impedance parameters of mild steel electrode in 0.5 M sulfuric acid in the presence of different concentrations of the Schiff base S_1 at temperature range of 298–318 K

T/K	C/ppm	Rs/Ω cm^2	$Y_{0\ (dl)}$/Ω cm^2 s^n	C_{dl}/μF cm^{-2}	R_{corr}/Ω cm^2	θ	$\eta_{\%Z}$
298	Bare	2.92	2.05E-04	0.903	20.27		
298	25	13.34	2.36E-04	0.895	49.16	0.5877	58.8
298	50	6.32	2.06E-04	0.905	61.41	0.6699	67.0
298	100	33.51	2.05E-04	0.910	67.06	0.6977	69.8
298	150	6.73	1.70E-04	0.918	69.59	0.7087	70.9
298	200	15.46	2.17E-04	0.874	69.84	0.7098	71.0
298	300	8.69	2.13E-04	0.900	74.15	0.7266	72.7
298	400	14.44	1.80E-04	0.916	79.51	0.7451	74.5
308	Bare	2.60	2.20E-04	0.918	16.79		
308	25	8.37	2.56E-04	0.938	22.96	0.2681	26.8
308	50	5.83	2.31E-04	0.936	23.19	0.2760	27.6
308	75	6.62	2.17E-04	0.937	24.42	0.3124	31.2
308	100	6.08	2.43E-04	0.935	26.78	0.3730	37.3
308	150	6.73	2.57E-04	0.938	29.77	0.4360	43.6
308	200	8.20	2.11E-04	0.932	33.2	0.4943	49.4
308	300	8.32	2.49E-04	0.928	35.2	0.5230	52.3
308	400	6.91	1.67E-04	0.942	39.6	0.5760	57.6
313	Bare	2.63	1.65E-04	0.917	15.54		
313	50	9.27	2.28E-04	0.932	16.92	0.0816	8.2
313	75	7.65	2.92E-04	0.924	17.77	0.1255	12.5
313	100	10.1	2.21E-04	0.920	20.36	0.2367	23.7
313	150	12.02	2.11E-04	0.928	25.68	0.3949	39.5
313	200	3.18	5.04E-04	0.935	30.76	0.4948	49.5
313	300	2.12	2.52E-04	0.928	35.27	0.5594	55.9
313	400	2.98	2.96E-04	0.918	48.69	0.6808	68.1
318	Bare	2.43	1.45E-04	0.927	12.49		
318	25	2.37	4.38E-04	0.898	13.82	0.0962	9.6
318	50	2.20	1.90E-04	0.939	17.37	0.2797	28.0
318	75	2.08	3.24E-04	0.917	20.26	0.3835	38.4
318	100	2.25	2.64E-04	0.925	22.02	0.4328	43.3
318	150	2.17	2.63E-04	0.938	30.4	0.5891	58.9
318	200	2.38	2.90E-04	0.924	32.58	0.6166	61.7
318	300	2.10	2.68E-04	0.929	37.84	0.6699	67.0
318	400	2.30	2.57E-04	0.929	37.99	0.6712	67.1

$$\eta_{\%p} = \frac{i_{corr_0} - i_{corr}}{i_{corr_0}} \times 100 \quad (3)$$

where i_{corr} and i_{corr0} are the corrosion current densities (μA cm^{-2}), respectively, for the inhibited and the uninhibited situations. It is clear that corrosion current density decreases with increasing concentration. The corrosion potential does not change markedly. Depolarization of both anodic and cathodic branches after addition of the inhibitors indicates that not only dissolution of metal, but also evolution of hydrogen and oxygen (we did not try to purge the dissolved oxygen out of the cell) were suppressed. So, the Schiff bases cause a decrease in steel corrosion rate in acid media by influencing both the anodic and cathodic reactions. The change in Tafel slope of the anodic branch β_a and cathodic branch β_c confirm this statement. Therefore, we can suggest that the behavior of these inhibitors is mixed.

3.3 Adsorption isotherms

The establishment of isotherms that describe the adsorptive behavior of a corrosion inhibitor is an important part of its study, as they can provide important clues to the nature of the metal–inhibitor interaction [18]. Several adsorption isotherms were assessed. The simplest, is the Langmuir

Table 2 Impedance parameters of mild steel electrode in 0.5 M sulfuric acid in the presence of different concentrations of the Schiff base S_2 at temperature range of 298–318 K

T/K	*C*/ppm	*Rs*/Ω cm^2	$Y_{0\ (dl)}$/Ω cm^2 s^n	C_{dl}/μF cm^{-2}	R_{corr}/Ω cm^2	θ	$\eta_{\%Z}$
298	Bare	2.92	2.05E-04	0.903	20.27		
298	25	4.34	2.53E-04	0.892	46.53	0.5644	56.4
298	50	4.46	1.68E-04	0.902	61.80	0.6720	67.2
298	75	4.30	2.76E-04	0.877	62.78	0.6771	67.7
298	100	6.30	2.18E-04	0.894	65.61	0.6911	69.1
298	150	4.44	2.32E-04	0.879	72.81	0.7216	72.2
298	200	4.36	2.47E-04	0.875	80.84	0.7493	74.9
298	300	5.47	1.45E-04	0.914	94.05	0.7845	78.4
298	400	4.85	1.97E-04	0.877	107.50	0.8114	81.1
308	Bare	2.60	2.20E-04	0.918	16.79		
308	25	2.28	2.11E-04	0.934	24.50	0.3147	31.5
308	50	2.36	2.15E-04	0.935	26.69	0.3709	37.1
308	75	2.26	1.50E-04	0.938	30.87	0.4545	45.5
308	100	2.34	1.69E-04	0.924	32.55	0.4842	48.4
308	150	2.16	2.35E-04	0.917	35.79	0.5309	53.1
308	200	2.57	1.38E-04	0.918	48.08	0.6434	64.3
308	300	2.46	1.19E-04	0.930	56.30	0.7018	70.2
308	400	2.37	1.23E-04	0.923	63.75	0.7366	73.7
313	Bare	2.63	1.65E-04	0.917	15.54		
313	25	2.66	2.19E-04	0.936	17.15	0.0939	9.4
313	50	2.52	2.36E-04	0.915	18.64	0.1663	16.6
313	75	2.57	2.11E-04	0.917	22.13	0.3552	35.5
313	100	2.45	2.24E-04	0.926	24.10	0.3977	39.8
313	150	2.30	1.78E-04	0.928	25.80	0.2978	29.8
313	200	2.23	1.38E-04	0.926	29.59	0.4748	47.5
313	300	2.29	1.73E-04	0.918	37.34	0.5838	58.4
313	400	2.66	1.36E-04	0.921	63.50	0.7553	75.5
318	Bare	2.43	1.45E-04	0.927	12.49		
318	25	2.06	3.15E-04	0.902	17.28	0.2772	27.7
318	50	1.97	2.72E-04	0.923	19.72	0.3666	36.7
318	75	2.14	2.05E-04	0.927	28.53	0.5622	56.2
318	100	2.25	3.01E-04	0.898	30.21	0.5866	58.7
318	150	1.99	2.27E-04	0.914	32.42	0.6147	61.5
318	200	1.877	5.48E-04	0.933	33.12	0.6229	62.3
318	300	2.357	2.34E-04	0.920	33.46	0.6267	62.7
318	400	2.161	3.51E-04	0.886	39.44	0.6476	64.8

isotherm, based on the assumption that all adsorption sites are equivalent and that particle binding occurs independently from nearby sites being occupied or not. Interactions between adsorbed species complicate the problem by making the energy of adsorption a function of surface coverage. One of the isotherms that include this possibility is the Temkin isotherm. The Temkin adsorption isotherm was found to provide the best description of the adsorption behavior of the Schiff bases; this has the following surface coverage, θ, and the bulk concentration, c, relationship:

$$f(\theta, x)\exp(-2a\theta) = kc \tag{4}$$

where $f(\theta, x)$ is the configurational factor, which depends on the physical model and the assumptions underlying the derivation of the isotherm, θ is the degree of surface coverage, x the size ratio, "a" the molecular interaction parameter, c the inhibitor concentration in the electrolyte and k is the equilibrium constant for adsorption.

The equation expressing Temkin's adsorption isotherm is:

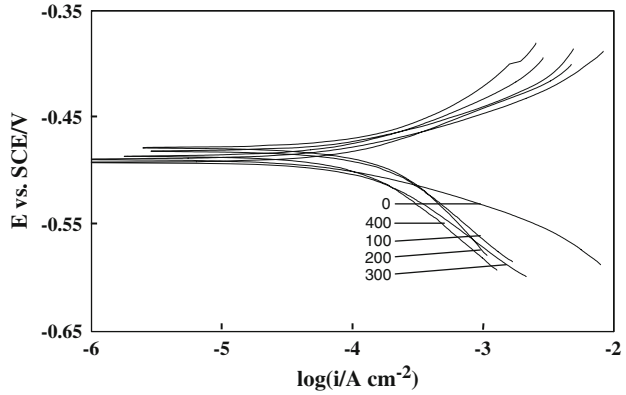

Fig. 5 Tafel polarization curves of mild steel in 0.5 M H_2SO_4 at 298 K; containing different amounts of the Schiff base S_1; (1) Bare, (2) 100, (3) 200, (4) 300, and (5) 400 ppm

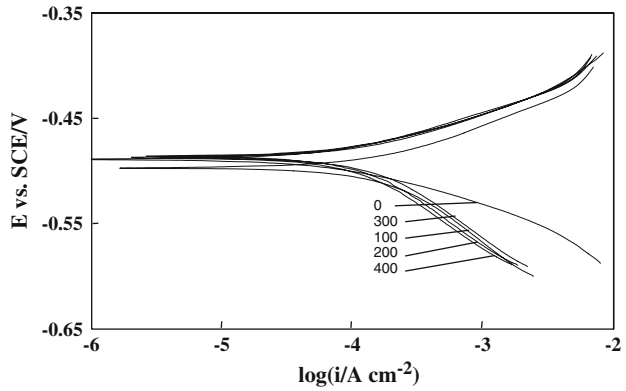

Fig. 6 Tafel polarization curves of mild steel in 0.5 M H_2SO_4 at 298 K; containing different amounts of the Schiff base S_2; (1) Bare, (2) 100, (3) 200, (4) 300 and (5) 400 ppm

$$k_{\text{ads}}C = e^{f\theta} \tag{5}$$

where k_{ads} is the adsorption equilibrium constant, θ is the degree of surface coverage, C is the molar concentration of inhibitor (mol L^{-1}) and "f" is the molecular interaction constant. The plots of ln$C$ against θ displayed a straight line for the inhibitors tested. The linear plot with high correlation coefficient (0.998 and 0.995 for S_1 and S_2, respectively) clearly revealed that the surface adsorption process of inhibitors on the mild steel surface obeys the Temkin adsorption (Fig. 7). The surface coverage θ can readily be calculated from the Eq. 5 as in that case it is numerically identical to the value of the inhibition efficiency: $\theta = \eta_{\%}/100$.

In order to study the effect of temperature EIS experiments were conducted at 298, 308, 318, and 325 K in 0.5 M H_2SO_4 solution in the presence of S_1 and S_2 at concentration 25–400 ppm. Corrosion characteristics obtained from the EIS curves are given in Tables 1 and 2. Inhibition efficiencies were found to decrease as temperature increased. To study the inhibitive mechanism, the amount of heat of adsorption is necessary. This can be calculated according to the Van't Hoff equation:

$$\ln k_{\text{ads}} = \left(\frac{-\Delta H^0_{\text{ads}}}{RT}\right) + \text{Const.} \tag{6}$$

where ΔH^0_{ads} and k_{ads} are the adsorption heat and adsorptive equilibrium constant, respectively. It should be noted that $-\frac{\Delta H^0_{\text{ads}}}{R}$is the slope of the straight line lnk_{ads} vs. $1/T$ according to Eq. 6. The standard adsorption free energy ΔG^0_{ads} was obtained according to [22–24].

$$k = \frac{1}{55.5}\exp\left(\frac{-\Delta G^0_{\text{ads}}}{RT}\right) \tag{7}$$

where ΔG^0_{ads} the free energy of adsorption, R is the universal gas constant and T the thermodynamic temperature, 55.5 is the number of moles of water in solution expressed in mol L^{-1}. The standard adsorption entropy $\left(\Delta S^0_{\text{ads}}\right)$ was obtained by the thermodynamic equation:

$$\Delta S^0_{\text{ads}} = \frac{(\Delta H^0_{\text{ads}} - \Delta G^0_{\text{ads}})}{T} \tag{8}$$

The thermodynamic parameters for adsorption obtained from the Temkin adsorption isotherms for the studied molecules are given in Table 5. Higher values were obtained for ΔH^0_{ads} in the presence of inhibitors,

Table 3 Tafel polarization parameters for the corrosion of mild steel in 0.5 M sulfuric acid containing different concentrations of the Schiff base S_1

C/ppm	I_{corr}/μA cm^{-2}	$-E_{\text{corr}}$ vs. SCE/mV	β_a mV/Decade	β_c mV/Decade	Θ	$\eta\%_p$
Bare	343.3	502	75	94	–	–
25	154.7	481	80	116	0.5492	54.9
50	140.9	474	93	147	0.5894	58.9
100	113.4	481	89	98	0.6697	67.0
150	102.0	491	42	120	0.7000	70.3
200	106.3	478	59	104	0.6901	69.0
300	92.2	492	59	85	0.7299	73.1
400	85.9	486	53	54	0.7498	75.0

Table 4 Tafel polarization parameters of the corrosion of mild steel in 0.5 M sulfuric acid containing different concentrations of the Schiff base S_2 at temperature range of 298–318 K

C/ppm	I_{corr}/μA cm^{-2}	$-E_{corr}$ vs. SCE/mV	β_a mV/Decade	β_c mV/Decade	Θ	η%
Bare	343.3	502	75	94	–	–
25	145.2	487	50	114	0.5769	57.7
50	136.9	486	50	107	0.6010	60.1
100	132.4	497	44	60	0.6142	61.4
150	122.3	496	48	69	0.6436	64.4
200	95.9	487	36	54	0.7205	72.1
300	67.1	489	34	64	0.8046	80.5
400	54.9	487	28	43	0.8402	84.0

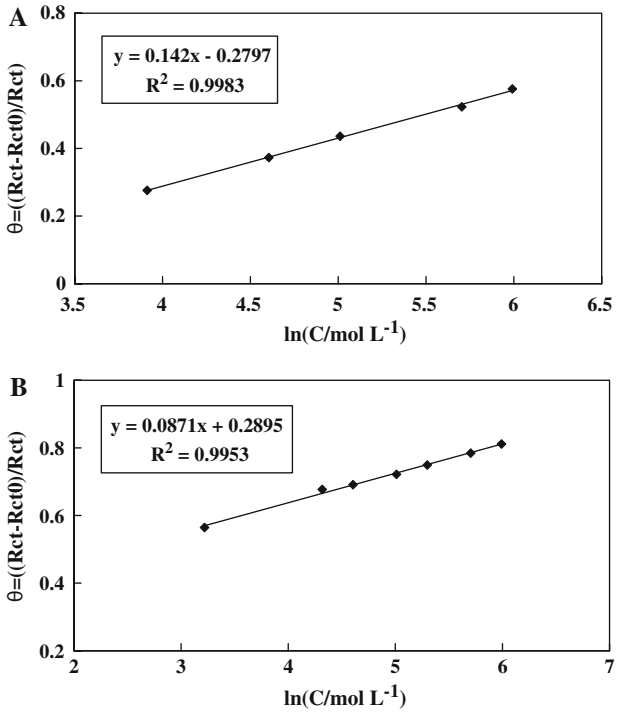

Fig. 7 Temkin adsorption isotherm plots of **a** S_1 **b** S_2 for mild steel in 0.5 M H_2SO_4 in the presence of different concentrations of the studied Schiff bases from impedance data

indicating the higher protection efficiency observed for these inhibitors. The calculated values of ΔG^0_{ads} are negative which indicates that adsorption is a spontaneous process. Generally, values of ΔG^0_{ads} around −20 kJ mol^{-1} or lower are consistent with the electrostatic interaction between charged molecules and the charged metal surface (physisorption); those around −40 kJ mol^{-1} or more negative involve charge sharing or transfer from organic molecules to the metal surface which form a coordinate type of metal bond (chemisorption) [23].

In the present work, the calculated ΔG^0_{ads} values are −56.12 and −77.43 kJ mol^{-1} for S_1 and S_2, respectively, at 298 K. These values less negative than −40 kJ mol^{-1} indicating the chemisorptions of inhibitor molecules. From Table 5, a limited decrease in the absolute value of ΔG^0_{ads} with increase in temperature is observed, indicating that adsorption is somewhat unfavorable with increasing temperature, and that physisorption has the major contribution while chemisorption has the minor contribution in the adsorption mechanism.

The ΔH^0_{ads} of inhibitors S_1 and S_2 are −179.96 and −492.61 kJ mol^{-1}, respectively, showing that the adsorption is an exothermic process [24]. In an exothermic process, physisorption is distinguished from chemisorption by considering the absolute value of ΔH^0_{ads}. For the

Table 5 Summary of fundamental adsorption constants of the inhibitor compounds

Schiff bases	*T*/K	ln(*k*)	ΔG^0_{ads}/kJ mol^{-1}	ΔH^0_{ads}/kJ mol^{-1}	ΔS^0_{ads}/J mol^{-1}K^{-1}
S_1	298	22.65	−56.12	−179.96	−415.60
	308	19.95	−51.09		−418.41
	313	19.18	−49.90		−415.53
	318	18.04	−47.68		−415.98
S_2	298	31.25	−77.43	−492.61	−1393.25
	308	25.19	−64.51		−1389.95
	313	21.00	−54.65		−1399.25
	318	19.12	−50.54		−1390.15

physisorption process $\Delta H^0_{ads}$is lower than 40 kJ mol^{-1} while that for chemisorptions process approaches 100 kJ mol^{-1}. All values of ΔS^0_{ads} are negative in the adsorption process; inhibitor molecules are adsorbed in orderly fashion onto the steel surface, causing a decrease in entropy [25]. As entropy decreases for any exothermic process, the larger values of ΔG^0_{ads} $\Delta H^0_{ads}$and ΔS^0_{ads} at each temperature for S_2, shows that the inhibitive action of the S_2, is better than S_1.

3.4 Inhibition mechanism

A clarification of the mechanism of inhibition requires full knowledge of the interactions between the protecting compound and the metal surface. Methods providing molecular scale information regarding orientation, adlayer morphology, etc. such as surface-enhanced Raman scattering and scanning tunneling microscopy are invaluable in this respect, but are beyond the scope of the present research. However, comparison of structural analogies for S_1 and S_2 enables us to propose similar models which, in any case, agree with the experimental data presented.

If one considers the structures of the investigated compounds (Fig. 1), several potential sources of inhibitor–metal interaction can be identified. In the case of both Schiff bases, there are the free electron pairs on N, S, and O, capable of forming a co-ordination π-bond with Fe. Furthermore, the double bonds in the molecule allow back donation of metal d-electrons to the π*-orbitals, which is a type of interaction that cannot occur, e.g., with amines. Third, π electrons from the aromatic rings may interact with the metal surface, and finally, especially in acidic media, electrostatic interaction is possible between the negatively charged iron surface (which may be brought about by specific adsorption of sulfate anions) and the positively charged inhibitor, following protonation of its basic functionalities. In the case of S_2, basically the same interactions can occur; with the difference that the nitro group is replaced with the methoxy group. It is known that mild steel has coordination affinity to sulfur, nitrogen, and oxygen containing ligands. All the Schiff bases have electronegative donor atoms N, S, O, and π electrons of four aromatic rings. Efficient adsorption occurs with one of these atoms or through π electrons of the aromatic ring or both of them. According to Tables 1 and 2, inhibitor efficiencies increase from S_1 to S_2**.** In the S_1 molecule the nitro group in the para position decreases the inhibition efficiency since it has electrophilic character and decreases the resonance of π electrons in the structure. In addition, the S_2 molecule has a methoxy group bounded to an aryl ring that increases the resonance of π electrons to facilitate adsorption. By comparison of thermodynamics parameters for S_1 and S_2 (Table 5) we can see that these values are more negative for S_2 than S_1, showing the better performance of S_2.

4 Conclusions

The corrosion behavior of mild steel was investigated in 0.5 M sulfuric acid solution with and without addition of various concentrations of Schiff bases at different temperatures, using potentiodynamic and EIS techniques:

Both of the studied Schiff bases are good inhibitors for mild steel corrosion in sulfuric acid solution, generating inhibition efficiencies in the order of 70% at a concentration of 300 ppm. The evaluation of anti-corrosive process by polarization resistance studies, indicating that both S_1 and S_2 behave as mixed inhibitors. For low concentrations, S_1 and S_2 are indistinguishable in performance. As the concentration increases, S_2 shows an increasing inhibitive advantage over S_1, which is attributed to the presence of the methoxy group bounded to the aryl ring which increases the resonance of π electrons to facilitate adsorption. The nitro group bounded to the para position (in S_1) has a negative effect on the inhibition efficiency. The adsorption of Schiff bases on mild steel in 00.5 M sulfuric acid obeys Temkin's adsorption isotherm. According to the increase in the absolute value for ΔG_{ad}, ΔH_{ad}, and ΔS_{ad} at each temperature, the inhibitive action of S_2 was found to be better than that of S_1.

Acknowledgments The authors acknowledge the financial support of the office of the Vice Chancellor in charge of research of Tabriz University. Also, the authors appreciatively acknowledge Dr. L. Sagatforoush for synthesizing and preparing the Schiff bases from Khoy Peyam-Nour University (PNU).

References

1. Fan HB, Fu CY, Wang HL, Guo XP, Zheng JS (2002) Br Corros J 37:122
2. Hosseini MG, Mertens SFL, Ghorbani M, Arshadi MR (2003) Mater Chem Phys 78:800
3. Yurt A, Balaban A, Ustun Kandemir S, Bereket G, Erk B (2004) Mater Chem Phys 85:420
4. Emreğul KC, Kurtaran R, Atakol O (2003) Corros Sci 45:2803
5. Ma H, Chen S, Niu L, Shang S, Li S, Zhao S, Quan Z (2001) J Electrochem Soc 148:B208
6. Hosseini MG, Mertens SFL, Arshadi MR (2003) Corros Sci 45:1473
7. Ehteshamzadeh M, Shahrabi T, Hosseini MG (2006) Appl Surf Sci 252:2949
8. Hosseini MG, Ehteshamzadeh M, Shahrabi T (2007) Electrochim Acta 52:3680
9. Agrawal YK, Talati JD, Shah MD, Desai MN, Shah NK (2004) Corros Sci 46:633
10. Shokry H, Yuasa M, Sekine I, Issa RM, El-Baradie HY, Gomma GK (1998) Corros Sci 40:2173
11. Li S, Chen S, Lei S, Ma H, Yu R, Liu D (1999) Corros Sci 41:1273

12. Emregul KC, Atakol O (2003) Mater Chem Phys 82:188
13. Arshadi MR, Hosseini MG, Ghorbani M (2002) Br Corros J 37:76
14. Hosseini MG, Ehteshamzadeh M, Shahrabi T (2006) Anti-Corros Method Mater 53:296
15. Ehteshamzadeh M, Shahrabi T, Hosseini MG (2006) Anti-Corros Method Mater 53:147
16. Shahrabi T, Tavakholi H, Hosseini MG (2007) Anti-Corros Method Mater 54:308
17. Saghatforoush LA, Ershad S, Karimi-Nezahad G, Aminkhani A, Kabiri M (2007) Polish J Chem 81:241
18. Özbey S, Temel A, Ancin N, Öztas SG, Tüzün M, Kristallogr Z (1998) New Crys Struct 21:3207
19. Chetouani A, Aouniti A, Hammouti B, Benchat N, Benhadda T, Kertit S (2003) Corros Sci 45:1675
20. Lgamri A, Abou El-Makarim H, Guebour A, Ben Bachir A, Aries L, El Hajjaji S (2003) Progr Org Coat 48:63
21. Quraishi MA, Ajmal M, Shere S (1995) In: 8th European symposium on corrosion inhibitors, Annali dell'Universita di Ferrara, p 291
22. Durnie W, De Marco R, Jefferson A, Kinsella B (1999) J Electrochem Soc 146:1751
23. Bentiss F, Lebrini M, Lagrenee M (2005) Corros Sci 47:2915
24. Martinez S, Stern I (2002) Appl Surf Sci 199:83
25. Mu G, Li X, Liu G (2005) Corros Sci 47:1932